Article

Journal of
Nanoscience and Nanotechnology
Vol. 14, 9152–9157, 2014
www.aspbs.com/jnn

Dry Spun 3D Woven Carbon Nanotube Anode Electrode for Li-Ion Batteries

Seongwoo Ryu[1], Yunkyoung Kim[2], Haeshin Lee[1,*], and Soon Hyung Hong[2,*]

[1] Department of Chemistry, Korea Advanced Institute of Science and Technology, 291 Daehak-ro, Yuseong-gu, Daejeon 305-701, Korea
[2] Department of Materials Science and Engineering, Korea Advanced Institute of Science and Technology, 291 Daehak-ro, Yuseong-gu, Daejeon 305-701, Korea

Although carbon nanotubes (CNTs) have extraordinary mechanical, thermal, and electrical properties, application of CNTs remains limited due to their unique nano-sized tubular forms. CNT electrodes have relatively high sheet resistance, which does not meet the industrial requirements of various electrode materials. Thus, there are still challenges for improving the performance of CNTs in real applications, particularly in terms of satisfying industrial requirements. In this study, to utilize CNTs in bulk scale electrode applications, we developed a dry spinning technique. The dry spinning technique is a solid state fiber spinning technique that provides an adjustable aligned structure. The dry spinning approach also offers a facile and inexpensive fabrication process, factors which are favorable for industrial scalability for fabricating electrodes. We demonstrate a multilayer stacking process for enhancing the performance for li-ion batteries. Multi-layer CNT textiles have low sheet resistance and a 3D woven structure provides high surface area. The fabricated 3D woven structured electrode delivers a higher reversible capacity of more than 400 mA hr/g with high cycle stabilities.

Keywords: Carbon Nanotube, Fiber, Li-Ion Battery, Anode.

1. INTRODUCTION

Carbon nanotubes (CNTs) have been studied widely for their extraordinary mechanical,[1] electrical,[2] and thermal properties.[3] Due to their exceptional properties and unique hexagonal sp2-bonded nano-tubular structure, CNTs are considered to have outstanding potential for many future applications. Recently, CNTs have gained recognition as a next generation candidate anode material for lithium ion batteries (LIBs). Over the past decade, LIBs have been widely used in mobile electronics. Although conventional LIB exhibits great performance, there are many challenges remained in LIB. Improving capacity and cycle performance of anode material is one the biggest challenge. Conventionally, graphite has been used as an anode material for LIBs due to its high conductivity and favorable structure for ion diffusion and intercalation.[4] However, the theoretical LiC_6 structure in graphite limits the specific capacity at 372 mA h/g and actual performance of capacity is degrading over cycles.[5] To overcome this limitation, many research groups have developed and invented CNT based anode electrodes, with varying success. Researchers have found that CNTs can store Li ions both inside and outside of the nanotubes.[6] Moreover, the interstitial spaces of CNT bundles provide enhanced ability to intercalate lithium ions.[7,8]

In this study, we developed a 3D woven structured dry spun CNT anode for favorable lithium ion intercalation. Although, CNTs have extraordinary properties, their nano-sized tubular form restricts the capacity to exploit these outstanding properties. The first step for using CNTs in practical bulk scale applications is fiber spinning. Previously, various fiber spinning processes such as solution based wet spinning processes[9–12] and solid state spinning processes[13–21] have been investigated. Among them, one of the most promising processes for obtaining scalable CNT fiber is the dry spinning process.[18–21] Compare to other processes, the dry spinning process is in many regards a close approximation of the conventional silk worm spinning process. Therefore it is most scalable, suitable and applicable to conventional solid state weaving fabrication.

*Authors to whom correspondence should be addressed.

 1533-4880/2014/14/9152/006 doi:10.1166/jnn.2014.10099

In this study, we developed a 3D woven CNT anode as a favorable lithium ion intercalation structure by using a dry spinning process.

2. EXPERIMENTAL DETAILS

Synthesis of vertically aligned CNT array and fabrication of 3D woven structure Vertically aligned CNT arrays were synthesized by a CVD process (Atech System). We synthesized CNT arrays with a 1 nm thick Fe film deposited on a 10 nm thick Al coated Si substrate. The Fe catalyst layer and Al buffer layer were deposited via thermal evaporation (Atech System). Forming gases, argon (Ar) gas, hydrogen (H_2) gas, and oxygen (O_2) gas, were used as a supporting gas, and ethylene (C_2H_4) gas was used as a carbon source. To synthesize the vertically aligned CNT array, the temperature was raised to 750 °C for 10 min. under a 2000 sccm Ar gas flow. Then, 60 sccm H_2 gas was added to the Ar gas for 5 min. Finally, 1000 sccm C_2H_4 gas and 1 sccm O_2 gas were added to the Ar gas and H_2 gas for 10 min. The CNT sheet was primarly spun horizontally from the vertically aligned array by use of a knife and attached to a copper electrode via ethanol spraying. This process was repeated 200 times, rotating 90 degrees each time.

Characterization Scanning electron microscopy (XL30SFEG, Philips) and transmission electron microscopy (JEM-3010, JEOL) were used to observe the microstructure of CNT arrays and the 3D woven CNT anode structure. With the transmission electron microscopy images, we further observed the number of walls and the diameters of the CNTs. A micro-force testing system (Instron 8848, Instron) was used to measure the mechanical properties of the 3D woven CNT anode. To test the tensile strength of the CNT anode, we used the micro-force testing system at a strain rate of 0.01 mm/sec for a 10 mm gauge length. A 4 point probe configuration system (CMT SR2000/AIT) was used to measure the sheet resistance of the CNT anode. Electrochemical measurements were performed with an automatic battery cycler system (WBCS 3000, WonATech), using a Swagelok type cell. The as is 3D woven CNT electrode was used for the anode. Li metal foil was used as a counter electrode and the electrolyte was 1 M $LiPF_6$ dissolved in a mixture of ethylene carbonate (EC)/ dimethyl carbonate (DMC) (1:1 by volume). The cells were assembled in an argon-filled glove box. Electrochemical performances were evaluated at a rate of 0.1 C in a voltage range of 0.01–3 V.

3. RESULTS AND DISCUSSION

We fabricated 3D woven CNT sheets by using a dry spinning process. First, we prepared a 10 nm thick Al buffer layer with a 1 nm Fe catalyst layer on a Si substrate. By controlling the chemical vapor deposition (CVD) synthesis time, the morphology of the vertically aligned CNT array was tuned. Figure 1(a) shows a schematic diagram of the process to prepare vertically aligned CNT arrays and Figure 1(b) shows corresponding SEM images. Due to Van der Waals interactions between CNTs, these arrays can be spun into a continuous single sheet by mechanical drawing. This drawn sheet has loosely packed aerogel structures, which provide a favorable structure for intercalation and deintercalation of Li ions. For the preparation of anode electrodes, this sheet is directly attached on a copper electrode. Then, with 90 degree rotation, these sheets are continuously woven on the electrodes. Figures 1(c) and (d) show a SEM image of a single layer CNT sheet and woven CNT sheets comprising 200 layers.

We prepared two different CNT array samples for anode electrodes. The performance of LIBs is often influenced by the morphology of CNTs including defects,[22] length[23] and diameter.[24] From previous studies, it is well known that the morphology of CNT arrays can be tuned by controlling the catalyst and the synthesis duration. The array length

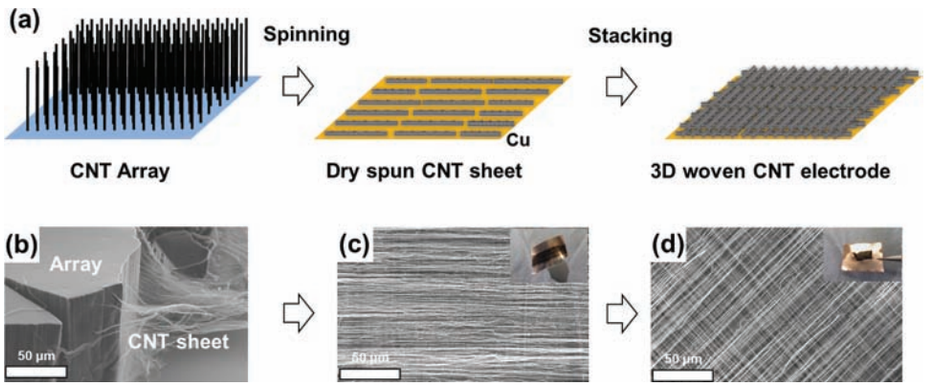

Figure 1. Fabrication and characterization of dry spun 3D woven carbon nanotube anode electrode. (a) Schematic diagram of aligned CNT arrays synthesized by a CVD process and (b) SEM images illustrating the dry spinning process of CNT fibers from the array. (c) Schematic diagram of aligned CNT arrays attached on a Cu substrate and a corresponding SEM image with a photograph (inset). (d) Schematic diagram of woven CNT arrays of 200 layers and a corresponding SEM image with a photograph of an electrode (inset).

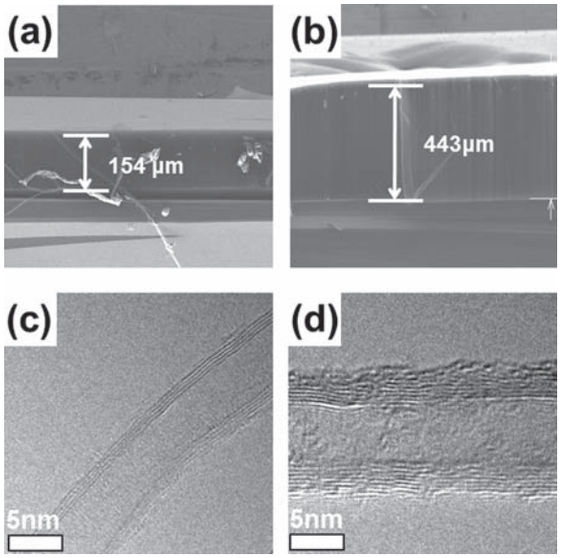

Figure 2. SEM images of vertically aligned CNT arrays (a) after 10 minute synthesis (CNT (S) and (b) 30 minute synthesis (CNT (L)). High resolution TEM images of CNTs after (c) 10 minute synthesis (CNT (S) and (d)) 30 minute synthesis (CNT (L)).

and diameters and the number of walls of the synthesized CNTs show different distributions according to the synthesis duration. This is due to migration of the Fe catalyst and the activation lifetime. We controlled the synthesis duration from 10 to 30 minutes with catalyst conditions of Al/Fe:10 nm/1 nm. Figure 2 shows SEM and TEM images of the CNT arrays after 10 minute synthesis and 30 minute synthesis. With 10 minute synthesis, we fabricated 154 μm arrays (Fig. 2(a)) with 7 nm diameter CNTs (Fig. 2(c)). These CNTs consisted mostly of double wall and triple wall structures. We refer to this array hereafter as CNT (s). With 30 minute synthesis, we fabricated 443 μm arrays (Fig. 2(b)) with 21 nm diameter CNTs (Fig. 2(d)). These CNTs consisted of more than 10 walls, thus indicating multi-walled structures. We refer to this array hereafter as CNT (L).

Before characterizing charge–discharge properties, we measured mechanical and electrical properties of different CNT anode electrodes. Electronic conductivity of anode material is important as a granular media in order to transport the electronic carrier from the current collector to the electrolyte. In other words, better electronic conductivity offers rapid transportation of the electronic carrier without losses to enhance the performance of LIB. For comparison with other CNTs, we prepared CNT bucky paper from conventional CNTs from Iljin Nanotech. The 3D woven CNT electrode performed displayed tensile strength (Fig. 3(a)), modulus (Fig. 3(b)), and elongation (Fig. 3(c)). The average tensile strengths were 213 MPa from CNT bucky paper, 698 MPa from 3D woven CNT electrode (s), and 798 MPa from 3D woven CNT electrode (L). The

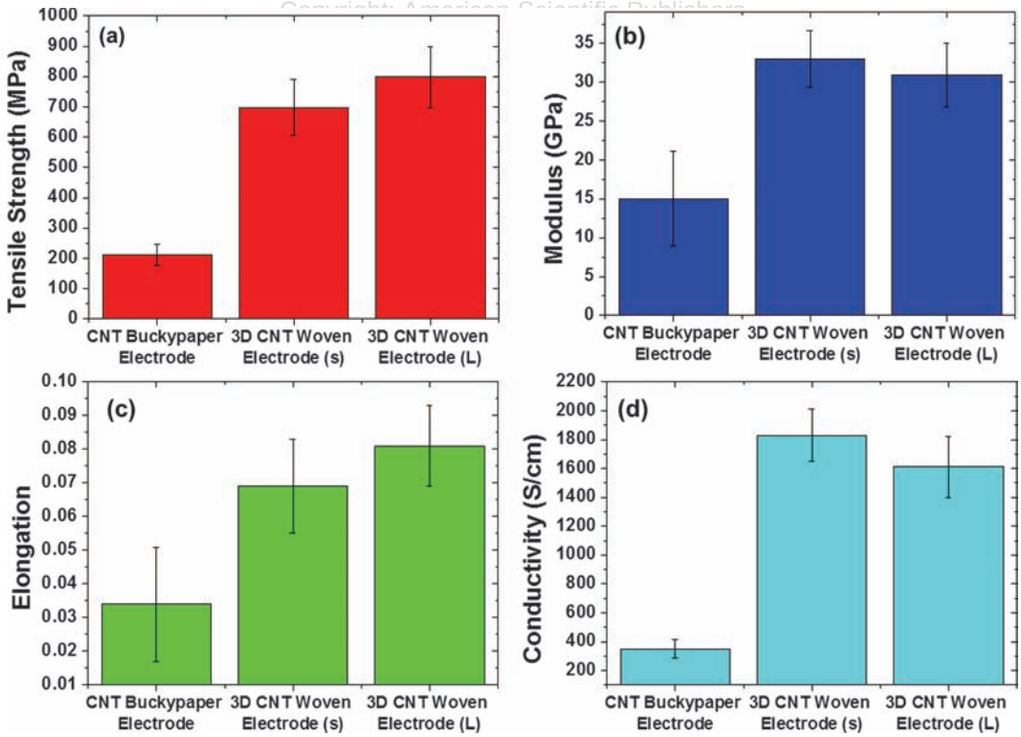

Figure 3. Mechanical and electrical characterization of CNT anode electrode. Conventional CNT (CN95 form Injin Nanotech) electrode fabricated by vacuum filtering, 3D woven electrode fabricated from CNT (s) and CNT (L). Comparison of 10 electrode samples of (a) tensile strength, (b) modulus, (c) elongation, and (d) electrical conductivities.

CNT bucky paper and 3D woven CNT electrode (s) and (L) exhibited an average modulus of 15 GPa, 33 GPa, and 31 GPa, respectively. Elongation of the 3D woven CNT electrode was increased from 0.034 (bucky paper) to 0.069 (3D woven CNT electrode (s)) and 0.081 (3D woven CNT electrode (L)). These results indicate that, compared to CNT bucky paper, load transfer was effectively distributed on the CNT woven electrodes. Furthermore, the aligned CNT nano-fabric structure minimized defects where stress concentration could occur. Bringing CNTs into an aligned structure also provides effective conductive paths in the anode electrodes (Fig. 3(d)). The conductivity of both 3D woven CNT electrode (s) and (L) exceeded 1500 S/cm, which is far greater than that of conventional bucky paper (350 S/cm). Generally, longer CNTs with a single wall structure exhibit higher conductivity characteristics when they are fabricated in the form of sheets. However, 3D woven CNT electrode (s) showed higher conductivity than (L). This is because CNT (L) has a multi-walle structure, which delivers higher electrical resistance properties than a single walled structure. Moreover, with longer CNT synthesis time, unreacted amorphous carbons are deposited

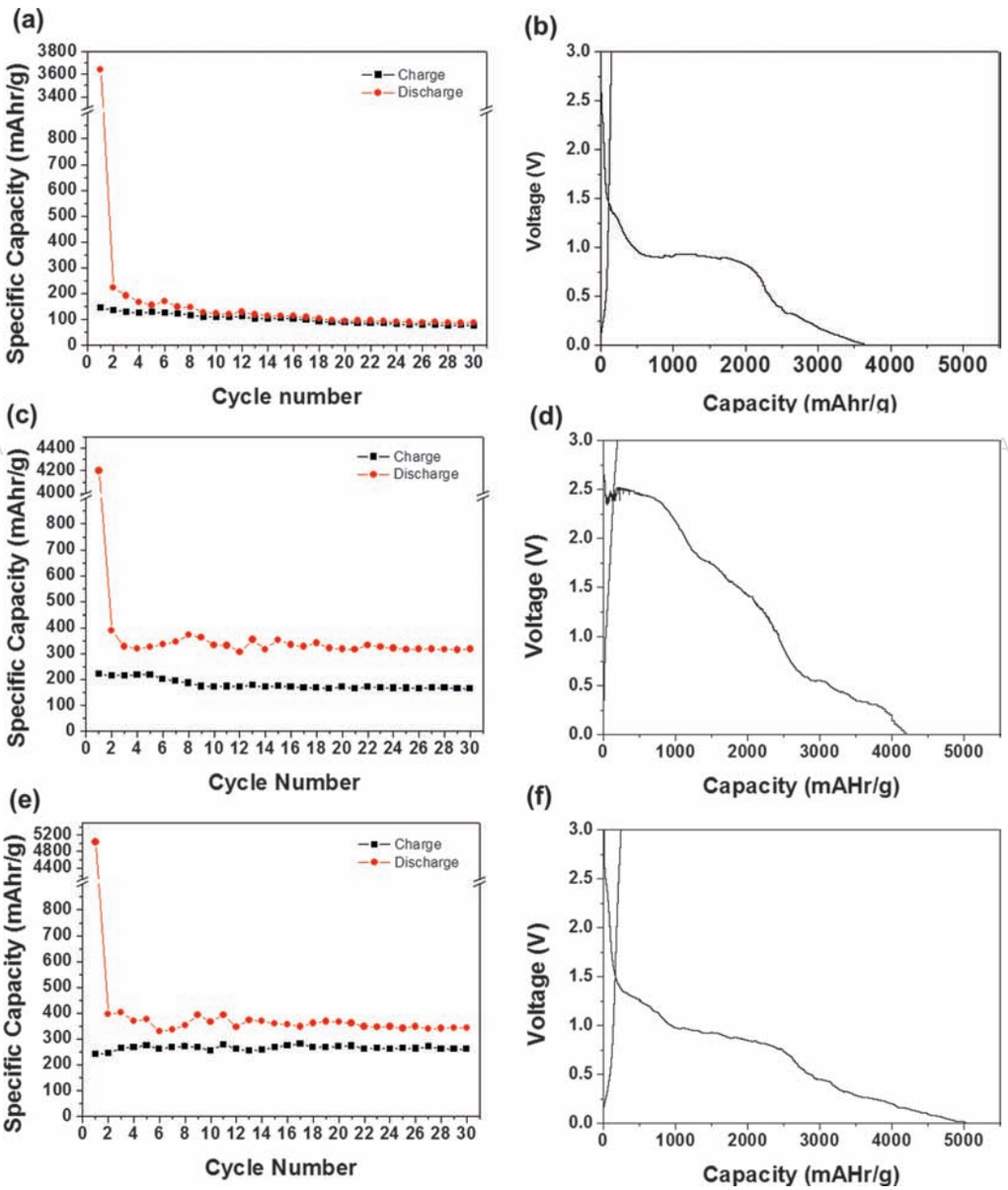

Figure 4. Characterization of electrochemical performance. (a) Cycling behavior of conventional CNT (CN95 form Injin Nanotech.) electrode and (b) their galvanostatic charge-discharge profiles in the 1st cycle. (c) Cycling behavior of 3D woven electrode fabricated from CNT (L) and (d) their galvanostatic charge–discharge profiles in the 1st cycle. (e) Cycling behavior of 3D woven electrode fabricated from CNT (s) and (f) their galvanostatic charge–discharge profiles in the 1st cycle.

on the surface of the CNTs, which increases contact resistance.

Charge–discharge characteristics of the coin cell were measured at the first cycle at a load current density of 0.02 mA/cm^2 between 0 and 3 V cutoff limits. Cyclic performance charge–discharge was monitored during 30 cycles. Figure 4 shows both the cyclic performance and the first cycle charge-discharge curve of CNT bucky paper an 3D woven CNT electrodes (L) and (s). The large differences in the morphology and structure of CNTs lead to different electrochemical performance when they are used as anode materials for LIBs. The CNT bucky paper displayed reversible capacity of 3640 mA h/g at the 1st cycle and the capacity continuously decreased from 222 mA h/g to 86 mA h/g from the 2nd to 30th cycle (Figs. 4(a) and (b)). Previously multi-wall CNT anodes also showed similar results that reversible capacity exhibited below 280 mA h/g.[25, 26] Compared to CNT bucky paper, 3D woven CNT electrodes (L) and (s) delivered almost twofold higher capacity values. 3D woven CNT electrode (L) displayed reversible capacity of 4200 mA h/g at the 1st cycle and its capacity stabilized between 390 mA h/g and 315 mA h/g, from the 2nd to 30th cycles (Figs. 4(c) and (d)). Whereas conventional CNT electrodes suffer from low practical capacities and high irreversible charge loss due to the formation of a solid electrolyte interface (SEI) and other side reactions,[27] these 3D woven CNT electrodes display both stable cycle performance and enhanced capacities. The aerogel structure of the woven electrode offers numerous storage sites for Li ions. Due to its enhanced mechanical properties, the woven structure also offers high structure resistivity during ion intercalations, which stabilizes the cycle performance of LIBs. 3D woven CNT electrode (s) showed slightly enhanced performance and displayed reversible capacity of 5030 mA h/g at the 1st cycle and the capacity stabilized between 401 mA h/g and 342 mA h/g, from the 2nd to 30th cycles (Figs. 4(e) and (f)). Both the diameter and the length of CNT (s) are smaller than those of CNT (L). Theoretically, lithium ions could intercalate outside and inside the CNTs. With an increase of the tube diameter, the intercalated lithium atoms tend to form a multi-shell structure at the inner-tubes, which improves the lithium capacity.[28] Because CNT (L) and CNT (s) have similar inner diameters, they do not provide an enhanced multi-shell structure. CNT (s), however, has shorter array length than CNT (L). This indicates that with same amount of CNTs, longer CNTs could provide similar storage sites but longer path ways to store Li ions. It is known that effective diffusion typically decreases if the CNTs are too long, since the Li ions are able to enter but seldom exit.[29] Consequently, CNT (s) showed higher capacity and it has been proven that woven electrodes with shorter CNTs are a more promising candidate than electrodes with longer CNTs as an anode material for LIBs. Still, both reversible capacity of 3D woven CNT electrodes were over 3600 mA h/g at first cycle which is 4 times higher than aligned CNTs reported before.[30] 3D woven structure displayed substantially great amount of capability because this structure itself provides enhanced sites between the layers for lithium absorption than only aligned structure. Beside storage sites 3D woven structure also has effective electrical path ways to the current collectors. Aligned CNT only serves 1D path ways through collectors but CNT electrode serves more than 1D path ways by intimate contact of 1D CNT bundles in rotation.

4. CONCLUSIONS

In conclusion, we demonstrated a dry spinning process to fabricate 3D woven CNT electrodes for application as LIB anodes. By exploiting Van der Waals interactions between CNTs, CNT arrays were spun into a 3D woven structure. We observed the correlation of the CNT woven structures with charge–discharge cycle performances. The 3D woven CNT electrode displayed maximum reversible capacity of 5030 mA h/g at the 1st cycle with stable cycling between 342 mA h/g and 401 mA h/g after the 30th cycle. The 3D woven CNT electrode proposed in this paper provides not only enhanced mechanical and electrical properties, but also favorable Li ion intercalation sites with cycle stability. The spinning principle proposed in this paper offers an entirely new way of fabricating next generation CNT based electrodes.

Acknowledgment: This work was supported from National Research Foundation of S. Korea: Biomedical Technology Development Program (2012-0000685, Haeshin Lee) and the Converging Research Center Program through the National Research Foundation of Korea (NRF) funded by the Ministry of Education, Science, and Technology (2011K000623, Soon Hyung Hong).

References and Notes

1. M. F. Yu, O. Lourie, M. J. Dyer, K. Moloni, T. F. Kelly, and R. S. Ruoff, *Science* 287, 637 **(2000)**.
2. A. Javey, J. Gue, Q. Wang, M. Lundstrom, and H. Dai, *Nature* 424, 654 **(2003)**.
3. M. F. Yu, B. S. Files, S. Arepalli, and R. S. Ruoff, *Phys. Rev. Lett.* 84, 5552 **(2000)**.
4. N. A. Kaskhedikar and J. Maier, *Adv. Mater.* 21, 2664 **(2009)**.
5. Z. G. Yang, J.-L. Zhang, M. C. W. Kintner-Meyer, X.-C. Lu, D.-W. Choi, J. P. Lemmon, and J. Liu, *Chem. Rev.* 111, 3577 **(2011)**.
6. J.-J. Zhao, A. Buldum, J. Han, and J.-P. Lu, *Phys. Rev. Lett.* 85, 1706 **(2000)**.
7. H. Shimoda, B. Gao, X. P. Tang, A. Kleinhammes, L. Fleming, Y. Wu, and O. Zhou, *Phys. Rev. Lett.* 88, 015502:1 **(2002)**.
8. B. Song, J. Yang, J. Zhao, and H. Fang, *Energ. Environ. Sci.* 4, 1379 **(2011)**.
9. B. Vigolo, A. Pénicaud, C. Coulon, C. Sauder, R. Pailler, C. Journet, P. Bernier, and P. Poulin, *Science* 290, 1331 **(2000)**.
10. L. M. Ericson, H. Fan, H. Peng, V. A. Davis, W. Xhou, J. Xulpizio, Y. Wang, R. Booker, J. Vavro, C. Guthy, A. N. G. Parra-Vasquez, M. J. Kim, S. Ramesh, R. K. Saini, C. Kittrell, G. Lavin, H. Schmidt, W. W. Adams, W. E. Billups, M. Pasquali, W. F. Hwang, R. H. Hauge, J. E. Fischer, and R. E. Smally, *Science* 305, 1447 **(2004)**.

11. A. B. Dalton, S. Collins, E. Muñoz, J. M. Razal, V. H. Ebron, J. P. Ferraris, and R. H. Baughman, *Nature* 423, 703 **(2003)**.
12. M. E. Kozlov, R. C. Capps, W. M. Sampson, V. H. Ebron, J. P. Ferraris, and R. H. Baughman, *Adv. Mater*. 17, 614 **(2005)**.
13. Y. L. Li, L. A. Kinloch, and A. H. Windle, *Science* 304, 276 **(2004)**.
14. K. Koziol, J. Vilatela, A. Moisala, M. Motta, P. Cunniff, M. Sennett, and A. Windle, *Science* 318, 1892 **(2007)**.
15. K. Jiang, Q. Li, and S. Fan, *Nature* 419, 801 **(2002)**.
16. L. Ci, N. Punbusayakul, J. Wei, R. Vajtai, S. Talapatra, and P. M. Ajayan, *Adv. Mater.* 19, 1719 **(2007)**.
17. L. Zheng, X. Zhang, Q. Li, S. B. Chikkannanavar, Y. Li, Y. Zhao, X. Liao, Q. Jia , S . K. Doorn, D. E. Peterson, and Y. Zhu *Adv. Mater.* 19, 2567 **(2007)**.
18. M. Zhang, K. R. Atkinson, and R. H. Baughman, *Science* 306, 1358 **(2004)**.
19. X. Zhang, K. Jiang, C. Feng, P. Liu, L. Zhang, J. Kong, T. Zhang, Q. Li, and S. Fan, *Adv. Mater.* 18, 1505 **(2006)**.
20. X. Zhang, Q. Li, T. G. Holesinger, P. N. Arendt, J. Huang, P. D. Kirven, T. G. Clapp, R. F. DePaula, X. Liao, Y. Zhao, L. Zheng, D. E. Petereson, and Y. Zhu, *Adv. Mater.* 19, 4198 **(2007)**.
21. X. Zhang, Q. Li, Y. Tu, Y. Li, J. Y. Coulter, L. Zheng, Y. Zhao, Q. Jia, D. E. Peterson, and Y. Zhu, *Small* 2, 244 **(2007)**.
22. K. N. Ishidate and M. Hasegawa, *Phys. Rev. B* 71, 245418:1 **(2005)**.
23. D. Zhang, Y. Zhao, J. B. Goodenough, Y. Lu, C. Chen, L. Wang, and J. Liu, *Electrochem. Commun.* 13, 125 **(2011)**.
24. N. Pierard, A. Fonseca, Z. Konya, I. Willems, G. van Tendeloo, and J. B. Nagy, *Chem. Phys. Lett.* 335, 1 **(2001)**.
25. S. Y. Chew, S. H. Ng, J. Wang, P. Novak, F. Krumeich, S. L. Chou, J. Chen, and H. K. Liu, *Carbon* 47, 2976 **(2009)**.
26. X. Li, J. Yang, Y. Hu, J. Wang, Y. Li, M. Cai, R. Li, and X. Sun, *J. Mater. Chem.* 22, 18847 **(2012)**.
27. S. Klink, E. Ventosa, W. Xia, F. La Mantia, M. Muhler, and W. Schuhmann, *Electrochem. Commun.* 15, 10 **(2012)**.
28. M. Zhao, Y. Xia, X. Liu, Z. Tan, B. Huang, F. Li, Y. Ji, and C. Song, *Phys. Lett. A* 340, 434 **(2005)**.
29. J. Y. Eom and H.-S. Kwon, *J. Mater. Res.* 23, 2458 **(2008)**.
30. D. T. Welna, L. Qu, B. E. Taylor, L. Dai, and M. F. Durstock, *J. Power Sources* 196, 1455 **(2011)**.

Received: 18 April 2013. Accepted: 6 January 2014.